

COMPARISON OF PULSE THERMOGRAPHY (PT) AND STEP HEATING (SH) THERMOGRAPHY IN NON-DESTRUCTIVE TESTING OF UNIDIRECTIONAL GFRP COMPOSITES

Paulina Kamińska • ORCID 0000-0002-3840-5615,
Jarosław Ziemkiewicz • ORCID 0000-0003-4982-6391,
Piotr Synaszko • ORCID 0000-0002-7884-0582,
Krzysztof Dragan • ORCID 0000-0003-1857-227X.

Air Force Institute of Technology, ul. Ks. Bolesława 6, 01-494 Warszawa, Poland

paulina.kaminska@itwl.pl, jaroslaw.ziemkiewicz@itwl.pl, piotr.synaszko@itwl.pl,
krzysztof.dragan@itwl.pl

ABSTRACT

This paper presents two techniques of active thermography i.e. the pulsed thermography technique and the step heating technique. The aim of this article is to compare these two techniques and present the possibilities, advantages and limitations of their use in the context of non-destructive testing of composite materials. The experimental section presents the results of tests carried out on samples of the polymer composites reinforced with glass fiber.

Keywords: pulsed thermography, step-heating thermography, composites, NDT, NDE, GFRP.

INTRODUCTION

There are various non-destructive testing methods and techniques used to detect material discontinuities without changing their properties. Non-destructive tests are used in many industry branches in view of the need to provide high quality products, equipment or constructions. The objects in the above mentioned testing techniques are various types of joints (welded, spot welded, soldered, glued, etc.), coatings and objects made of composite materials [1].

Due to economic concerns, in the aviation industry, aircraft frequently remain in service despite their decommission date. Extending the service time in terms of both calendar (number of years) and hourly (total flight time) requires assessment of the technical condition of the aircraft structure. Therefore, non-destructive testing is an important element of the process of increasing aircraft service life. In aviation, structures

are designed to achieve specific high mechanical properties with as lowest weight as possible. Thus, aircraft structures are being made of fiber-reinforced composite materials.

Composite materials are materials made of two or more components. One of them is the matrix while the rest play the role of reinforcement. This combination creates a structure which properties (e.g. mechanical, thermal, etc.) are usually better than the properties of individual components. In aviation, the reinforcement generally occurs in the form of unidirectional fibers [2].

Due to the specificity of the structure of composite materials, traditional methods of non-destructive testing (e.g. radiographic, ultrasonic) may be ineffective in detecting internal damages. This generates interest in other methods that may be more effective in this type of application. The difference in the thermophysical parameters between composite material components and damages occurring in them, allows for the effective application of infrared thermography techniques [3].

Thermography is a method of recording a series of images, based on the detection of radiation in the infrared spectrum. The result of the test is the conversion of this radiation into a visible image (thermogram). It enables observation and assessment of temperature distribution and their values on the external surface of the tested object [4]. Many typical defects that are objects of thermographic tests can be considered as thin gas gaps filled with air, which thermophysical parameters differ from those typical of solid materials being the subject of non-destructive testing [5].

Non-destructive testing using infrared thermography can be divided into two types: passive and active. The crucial difference between these two methods is that the active method uses an additional, external source of thermal stimulation of the object (heating or cooling), while in the passive method the test object is characterized by the temperature field which emits the radiation received and measured with a thermographic camera [3].

In this research, two techniques of active infrared thermography, i.e. pulse thermography and step-heating thermography, were used to examine the composite specimen and to assess the damage introduced. Based on the results, the possibilities and limitations of pulse and step-heating thermography were analyzed and compared.

Active Infrared Thermography

The main difference in active thermography procedures compared to passive ones is an additional source of thermal stimulation (heating or cooling) of the object. Damages of materials that have homogeneous temperature before the testing, most often equal to the ambient temperature, do not generate 'useful' temperature signals and for this reason require heating of the entire tested object or its part. During the test, heating creates a dynamic temperature field, and the results mainly depend on the observation time. Active thermography methods offer a wide range of analysis of the material structure disturbance and can be used for testing laminates, sandwich-structured composites and bonded structures. Thanks to these methods subsurface damages caused by impacts such as delamination and technological defects can be effectively detected [3, 6].

Active methods are classified according to the relative position of research devices, type of source, thermal stimulation or the shape and dimensions of the heat stimulation zone and temperature registration. Active thermography involves heating stimulation

of the test object and collecting thermograms (thermal images) as a function of time. Measurement of temperature distribution can be carried out both on the stimulated side (reflection method) and on the opposite side (transmission method) [3].

According to the type of stimulus and the method of processing and analysing thermographic data, the active thermography techniques fall into the following categories: pulsed thermography, step-heating thermography, lock-in thermography with modulated heating, and vibrothermography [7]. In the modulation method, the tested object is stimulated by a harmonic heat flux generated by a heating lamp. Thermal excitation is sinusoidal and based on the known frequency of the excitation signal and the recorded response of the system, its amplitude and phase shift angle. In the vibrothermographic method, the source of excitation is ultrasonic waves with a frequency range of 10- 20 kHz. The object's response to such excitation is a heat wave originating from a defect, recorded by a thermal imaging camera [3, 7].

Pulsed thermography

The pulsed thermography method is one of the most popular methods currently used in non-destructive testing of composite materials. This type of research involves using a lamp to generate a pulse (or a series of pulses) of thermal excitation that lasts from several milliseconds for materials with high thermal conductivity (e.g. metals) to several seconds for materials with low thermal conductivity. After switching off the radiation source, the object automatically cools down to the ambient temperature [8]. During the cooling phase, the temperature distribution on the surface of the tested object is determined and subjected to analysis (recording of thermograms). Due to the thermal parameters of the examined material structure and the defects below the surface, on the surface there are visible areas under which the material defects may occur. The limitation of this technique is the fact that absolute contrast rapidly disappears with depth of the defect. This limitation results from the difference in temperature of the defective area and the non-defective area. At the same time, it allows to detect defects, especially close to the surface [5].

Step-heating thermography

In contrast to pulsed thermography, step heating is the method that uses a long heating pulse so for thermal stimulation a much lower energy density is used. Relatively slow heating allows testing multi-layer structures and evaluating joints between the layers, detecting hidden corrosion in complex aircraft structures, and characterizing layer thickness. In addition, in step-heating thermography, changes in the surface temperature distribution are monitored during both the entire heating and the cooling process [8].

Detection of delamination by pulse thermography and step-heating thermography

In both techniques, the presence of defects in the material locally changes the thermal diffusivity, causing differences in temperature between the area containing the defect and the area free of material discontinuities. Defects detected are inclusions and delaminations which can be assessed by plotting the relations $\ln[T(t)-T(0)] = f[\ln(t)]$ (Figure 1). For a homogeneous material without defects, the cooling / heating curve is

a straight line with an absolute slope of 1/2. The temperature distribution is determined based on the temperature value on the surface of the material in the area without damage (T1) and in areas with damage (T2, T3, T4) [5, 10].

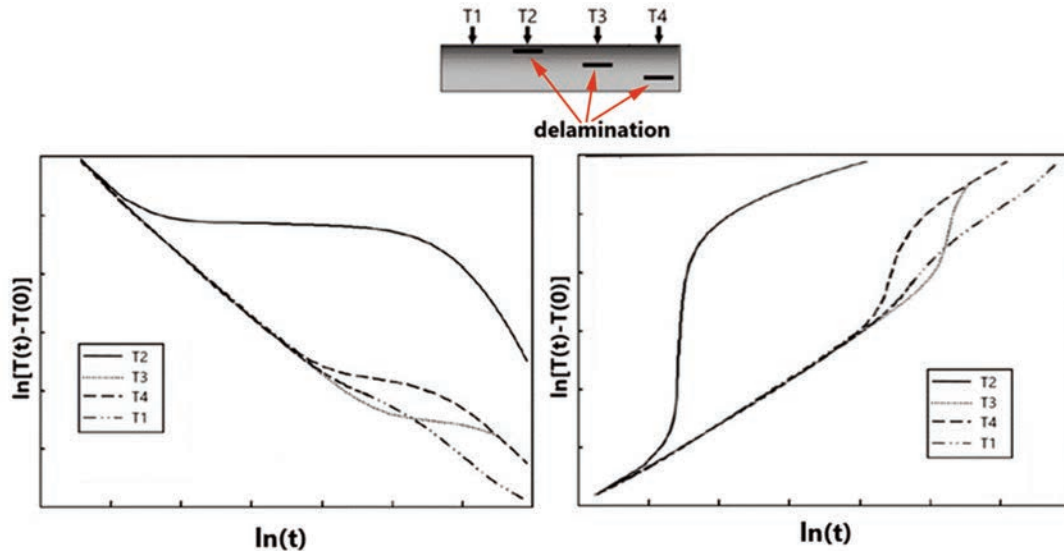


Figure 1. Detection of delamination by pulse thermography and long pulse thermography.

Detection of damage is possible after the minimum time has elapsed when differences in temperature values appear. The range in which the temperature difference is visible on the diagram lasts until the temperature stabilizes in the test area. Deeper damages require more heat and longer recording time. The detection of damage depends on the size and depth of the damage deposition. Therefore, the results obtained may be affected by an error. Thermography is a surface method, that is why it may not be possible to accurately determine the extent of damages that are deep inside the material [5].

EXPERIMENTAL TESTING

Testing specimen

According to the scope of this research a specimen from GFRP was tested. The tested specimen with dimensions 205 x 205 x 4.5 mm was made of TC E720 pre-preg. Artificial damages were entered into the sample in the form of sixteen flat-bottomed round holes (Figure 2) with different diameters and at different depths. Such a system of discontinuities makes it possible to check how the depth variation and the size of defects affect the received indications. Damages are identified by the letters A, B, C or D indicating the depth of the hole and a number specifying the diameter of the hole.

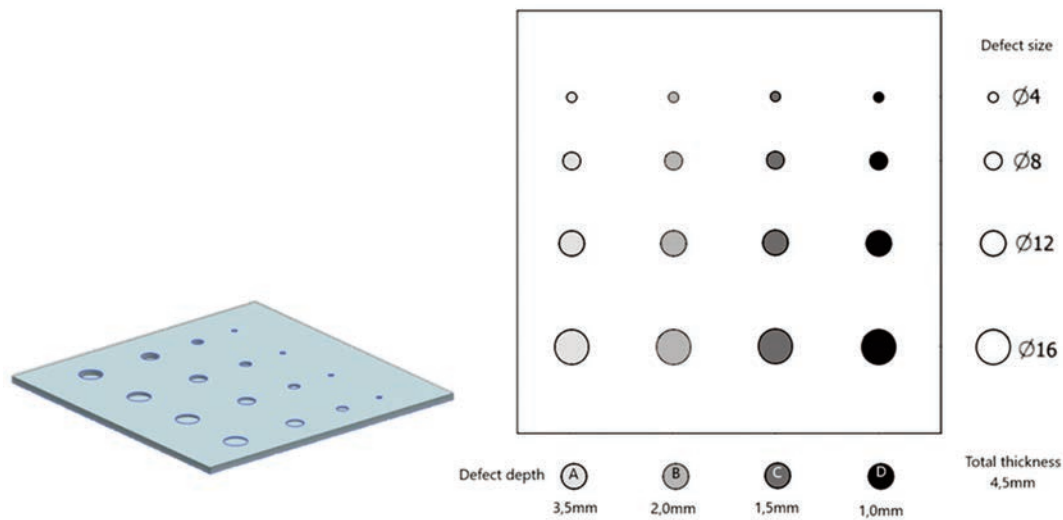


Figure 2. Sample of a GFRP with 16 flat-bottomed holes.

Methodology

For the examination of the specimen two types of active thermography techniques were used: pulsed thermography and step-heating thermography.

Pulse thermography was carried out using the Echo Therm System [10]. The apparatus creates a sequence of thermographic images, recording the temperature change of the tested surface within a specified time (in this case the time was 22s). The system is equipped with a FLIR SC7000 thermal imaging camera, two xenon (flash) lamps generating a total of 5kJ of thermal energy and software supporting the analysis that allows drawing temperature curves.

For step-heating thermography, the C-CheckIR system was used. The system is equipped with a halogen lamp with a much lower power than in the pulsed thermography system. The lamp power is 2kW @ 230V. Less energy supplied to the specimen surface during thermal excitation causes slower heating of the sample. Therefore, changes in the surface temperature distribution can be recorded both during the heating and during the cooling process. The time for heating and data collection was selected experimentally: 25s/10s, 30s/12s, 40s/16s (image recording time/sample heating time). The thermogram that gave the largest number of indications of damage was analyzed. The parameters of the cameras used for the particular techniques are presented in Table 1.

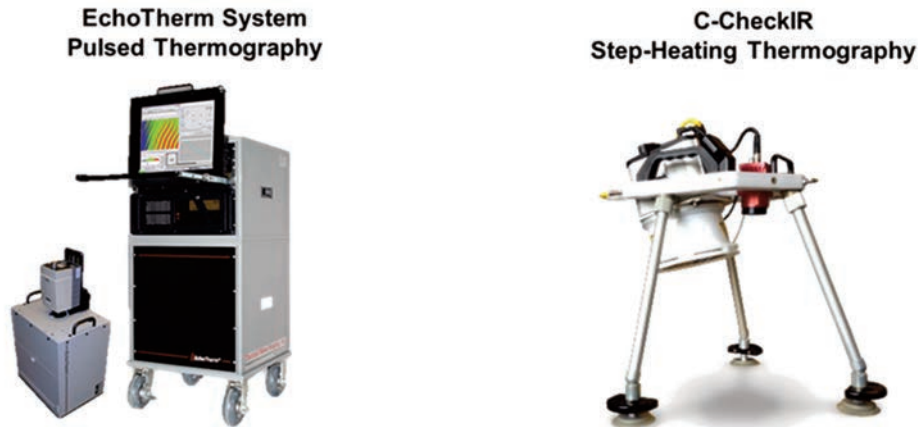


Figure 3. Pictures showing the measurement systems used.

Table 1. Parameters of infrared cameras.

Parameters	FLIR SC7000 EchoTerm	IRS-320S-NDT C-Check IR
Resolution	320x256 pixels	320 x 256 pixels
Spectral range	1,5-5,1 um	7,5-13 um
Sensitivity	2 mK	<30 mK
Frequency	Max 383 Hz	9 Hz

Processing of thermographic images

The mechanisms of TSR (Thermographic Signal Reconstruction) were used in the process of analysis of the obtained sequences. Digital processing of thermograms aims to improve the quality of the images obtained by removing interference caused by the background and the effect of the source of excitation and by sharpening structures of interest (e.g. cracks in laminate coatings, heterogeneity in the construction of materials).

For the analysis of the thermogram sequences obtained in the pulsed thermography, the temperature curves (temperature distribution on the surface of the tested object) were drawn with the aid of the software. The maximum temperature difference between the defected area and the undamaged areas often decreases, leading to equilibrium. This makes it impossible to observe temperature anomalies. The system allows the analysis of the surface temperature changes in logarithmic coordinates and the first and second temperature derivative.

Derivatives of the temperature logarithm function are useful especially in distinguishing areas of a defective structure from an undamaged structure. Image recording in the pulsed thermography begins immediately after extinguishing an excitation pulse. The results of thermographic tests are presented at different times, in a way that the indications of damage at a given depth are most visible [11]. To select the most appropriate time, the diagram of the specimen's cooling surface was used. For each image of the sequence, the contrast

and moment of image recording were selected individually, relative to the visibility of the observed damage. The aim was to obtain an image showing areas with damages at individual depths.

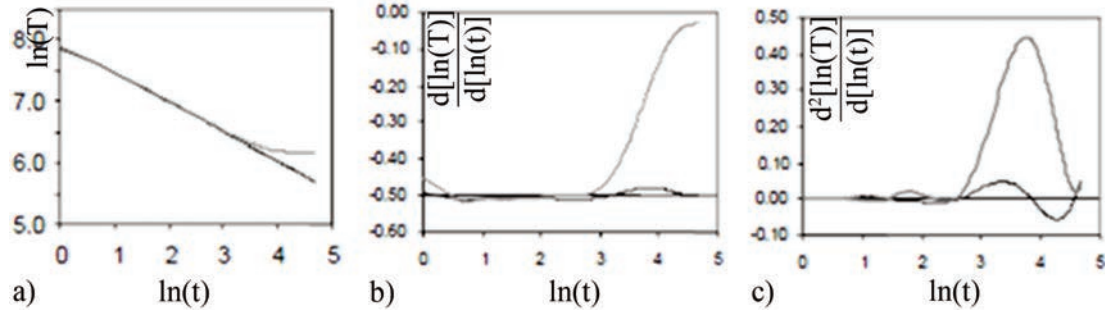


Figure 4. Change in surface temperature in TSR logarithmic coordinates [5]
a) Cooling process of the sample surface in logarithmic coordinates, b) Cooling process of the sample surface in logarithmic coordinates for the first derivative, c) Cooling process of the sample surface in logarithmic coordinates for the second derivative.

By means of step-heating thermography it is not possible to draw cooling curves and images in the first and second derivative using C-CheckIR system. Therefore, the researchers selected the thermograms that fit into the criterion of revealing the largest number of detected damages.

RESULTS

Analysis of thermograms

Thereafter, the analysis of the cooling curves of the tested sample surface in logarithmic coordinates is presented (Figure 5). In the diagram, the different colors of the curves correspond to individual areas on the sample. Five of them are in areas without damage. The rest were placed in areas of discontinuities at various depths. All markers were placed on damage with a diameter of 16mm. The damage located on the right side of the thermogram and marked pink (Figure 4d) is closest to the examined surface. The damage marked with navy blue, located on the left (Figure 4d), is the most distant from the examined surface.

Based on the cooling curves, the time moments (Table 2) were determined. There are noticeable differences in temperature values (marks B, C, D and E in Figure 5 a-c)). These time moments, on the cooling curves diagram for the second derivative (Figure 5c)) correspond to the maximum values of the peaks on the curves. These peaks correspond to damage at individual depths. The closer to the tested surface a damage is, the sooner the peak occurs. Therefore, the indication of damage on the thermogram can be observed after a shorter period of time.

In the diagram of the first derivative, it was possible to determine only one point (marked by A letter) for the damage closest to the test surface. This point corresponds

to the moment of time in which the minimum temperature change rate occurs in a given area. To obtain similar peaks for areas with damage at other depths, the test time should be extended.

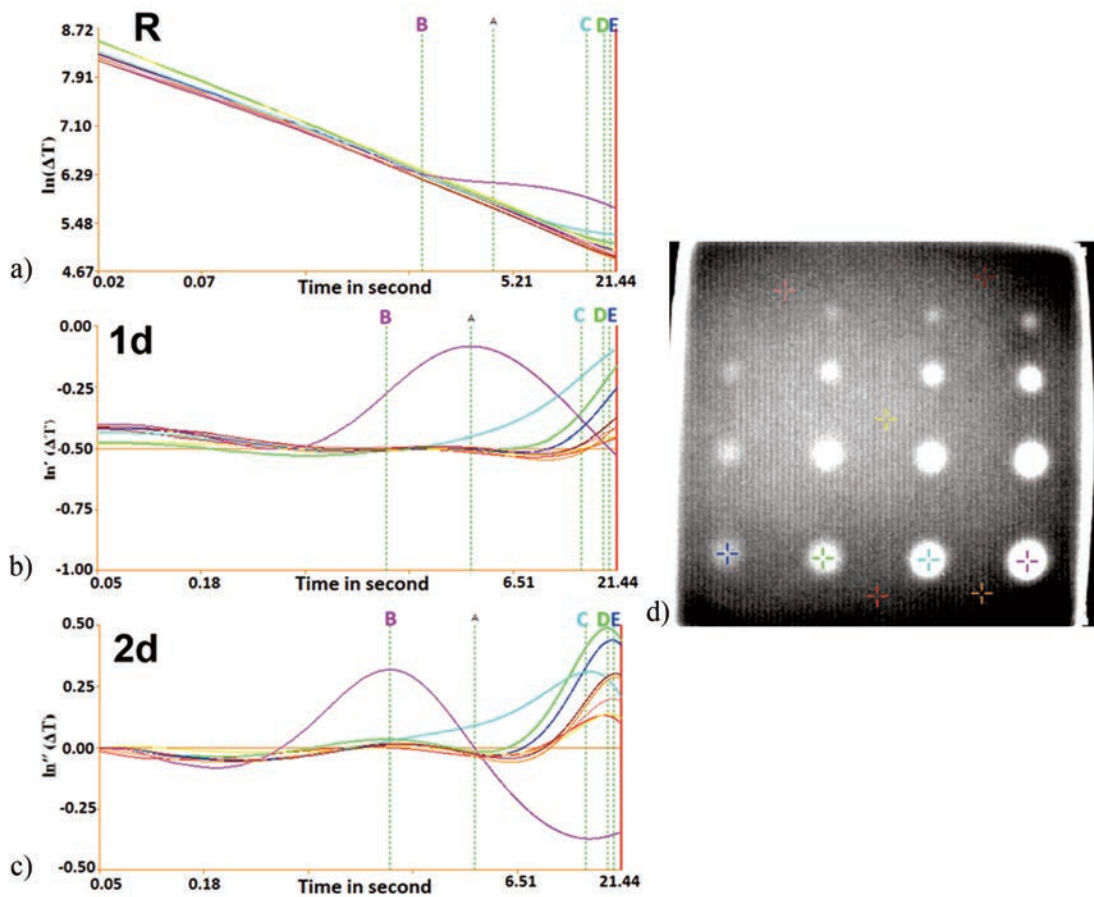



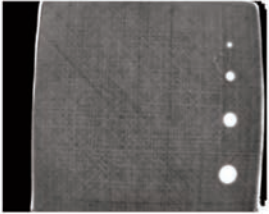
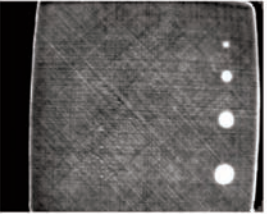
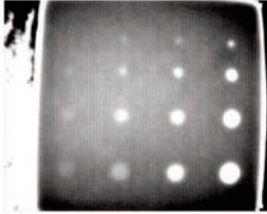
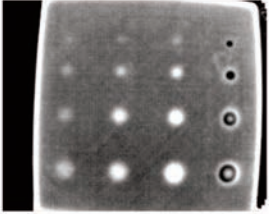
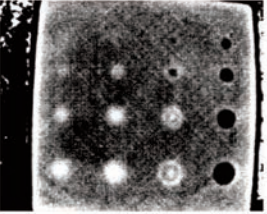
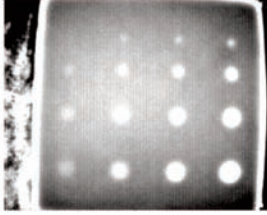
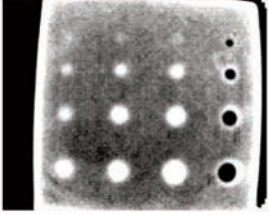
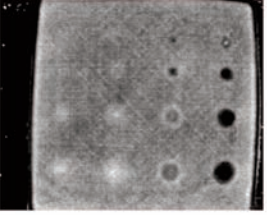
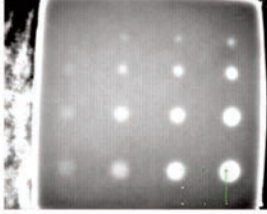
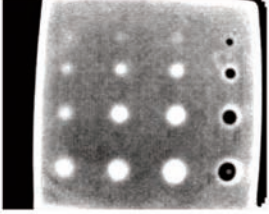
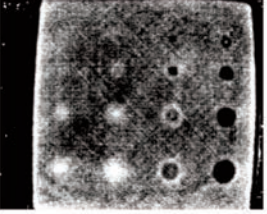
Figure 5. Thermographic measurement of a GFRP composite plate
a) Cooling diagram of the sample surface in logarithmic coordinates, b) Cooling diagram of the sample surface in logarithmic coordinates for the first derivative, c) Cooling diagram of the sample surface in logarithmic coordinates for the second derivative, d) Thermogram used to determine the cooling diagrams.

Table 2. Time moments corresponding to the characteristic points on individual diagrams.

MARK	R	1d	2d
B	1,535 s	3,948 s	1,535 s
C	14,384s	No indication	14,384s
D	17,911s	No indication	17,911s
E	19,026s	No indication	19,026s

Table 3 contains thermograms that are the results of mathematical transformation software that affect the contrast and accuracy in assessing the structure of the examined object. The thermograms were obtained at the times determined from the cooling curves.

Table 3. The results of thermographic tests using the pulsed thermography.

	R	1d	2d
1,535s			
14,384s			
17,911s			
19,026s			

Based on the images received, it can be observed that all indications of damages are round, which is consistent with the design requirement. The differential temperature contrast between damaged areas and areas without defects presents damage depth. The defects located just below the surface cause an increase in surface temperature, characterized by greater intensity of infrared radiation. The difference is noticeable both on the thermograms (Table 3) and on the diagrams of the temperature change over time (Figure 5). The application of first and second differentiation (Figure 5b-c) significantly affects the quality and accuracy of the analysis of the thermograms obtained.

In process of time, both the raw images and the differentiated thermograms show an increasing number of indications of damages located deeper below the test surface. However, the first seconds of the test images have better contrast. This is the result of the signal to noise ratio (SNR) decreasing over time. Therefore, damages closer to

the surface, regardless of their size, are clearly visible. It allows relatively accurate determination of the size of the damage. The edges of deeper damages are significantly more blurred. In consequence, the smallest damages may not be visible at all, and determining their size can be highly difficult. In addition, the results of such measurement are burdened with a greater error.

The system used in step-heating thermography did not allow for determining the temperature dependence on time. Therefore, the test parameters (total observation time / time of sample excitation) were selected experimentally in order to detect the largest number of damages. Three thermograms obtained using three different sets of parameters are presented below. As the observation of cooling curves was impossible only one thermogram that showed the largest number of indications of damages was selected out of each measurement. All thermograms were recorded during sample cooling.

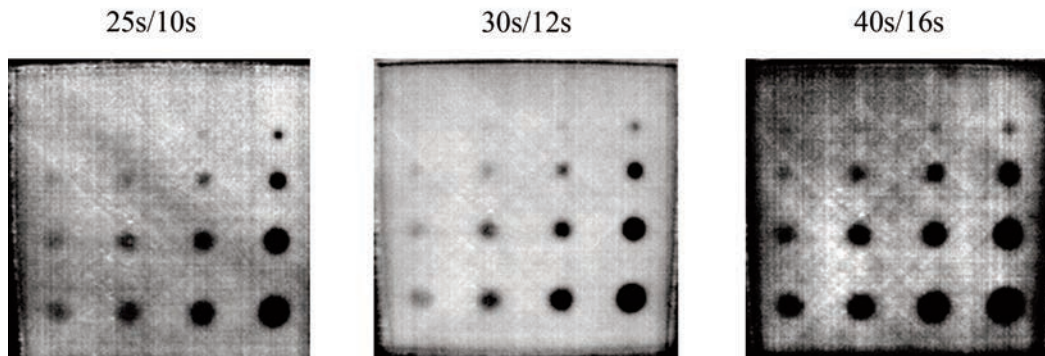


Figure 6. The results of thermographic tests using the step-heating thermography for various measurement parameters (total image recording time / heating time).

Unlike in pulsed thermography, in step-heating thermography the recorded image of the cooling of the sample during the first seconds does not show high contrast. More time for sample observation allows detecting better quality indications of damages. In step-heating thermography, longer heating stabilizes the images (increasing the signal-to-noise ratio SNR) and enables finding more damages. But, even without differential image processing, it is possible to observe damages located deep in the material.

Analysis of the obtained thermograms shows that damages are best visible over the longest heating time of the sample. Indications of damages in this thermogram have similar sizes in all rows despite being at different depths from the test surface. Moreover, compared to the pulsed technique, the edges of the defects are not blurred. This makes it easier to determine where the damage is located in the sample and what size it is. A number of damage indications is the same for both techniques.

IMAGE PROCESSING

The next stage of the study was to carry out an analysis that allows a quantitative description of damages. All thermograms obtained during pulsed and step-heating thermography are greyscale images (Figure 7a) where each pixel is described with one

of 256 shades of grey. The value 0 indicates black and 255 indicates white. These values were decoded using Scilab and exported to Excel (Figure 7b). Then the average value and standard deviation were calculated from the obtained data. In the next step the image was binarized using the three-sigma rule (Figure 7c). In order to illustrate the results received well, for both the grayscale images and the images after binarization the matrixes values were presented using colors and three-dimensional charts (Figure 7d, e). It is obvious that binarization allows the unambiguous separation of undamaged areas from areas with defects.

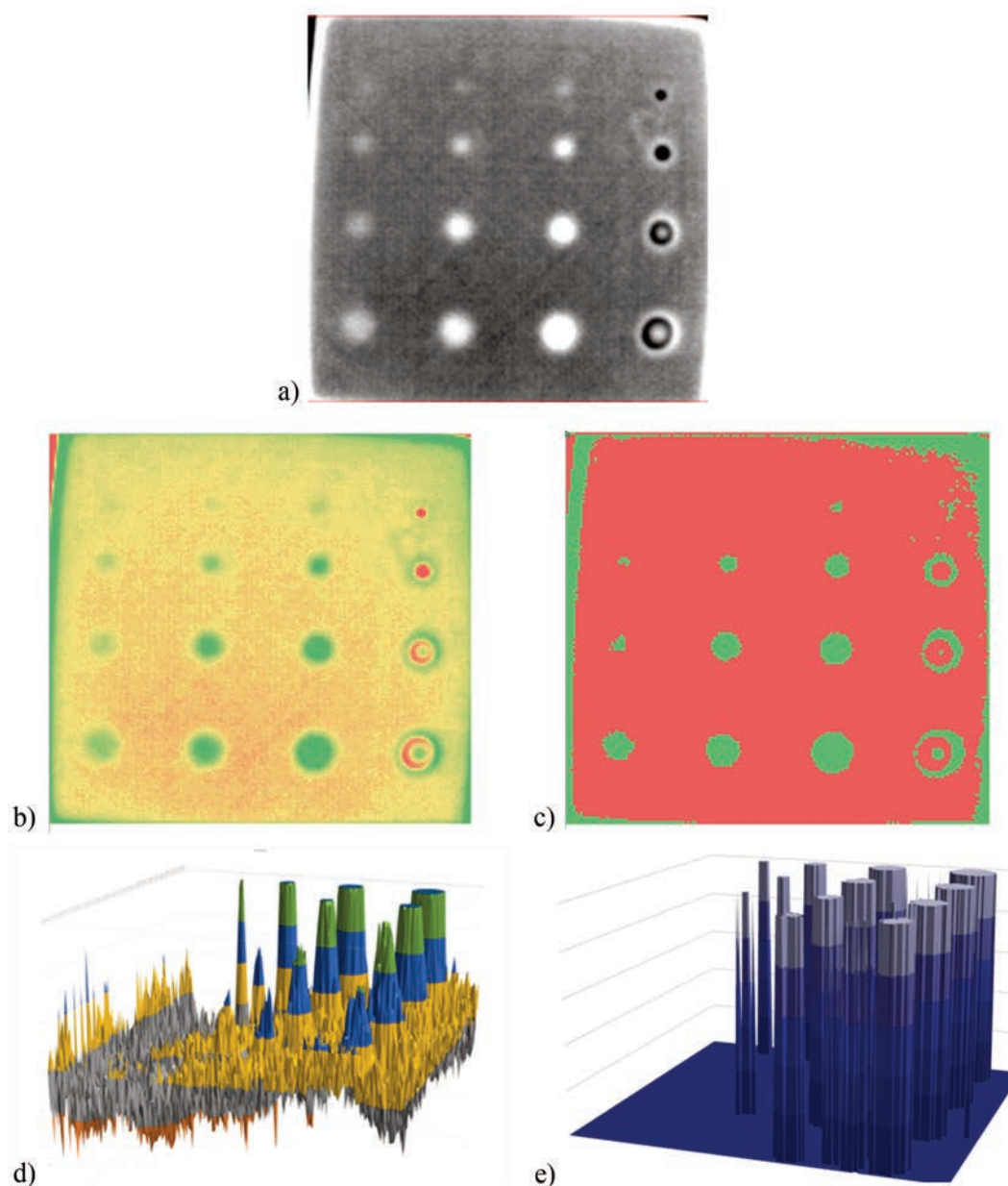


Figure 7 a) Thermogram, b) matrix obtained using Scilab, c) three-dimensional representation of matrix values, d) matrix after binarization, e) three-dimensional representation of the matrix after binarization.

For the pulsed thermography technique four thermograms were selected. They were created as a result of image processing by first order differentials. For step-heating thermography, analysis was carried out for three thermograms obtained from the measurements using different parameters. The next stage was to determine the size of individual defects based on the binarized images. Finally, for step-heating thermography, the damages' sizes were measured based on image which after binarization showed the largest number of damages (Table 4). The image from measurement 3 was selected (Table 4).

Table 4. The number of damage found after image binarization.

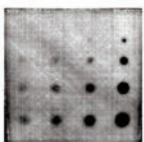


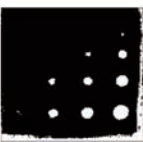
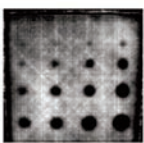
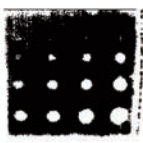
Measurement	Total data collection time / heating time	Thermogram	Image after binarization	Number of detected damages
1	25s/10s			9
2	30s/12s			10
3	40s/16s			14

Table 5. Results of analysis of images after binarization.


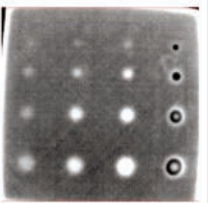
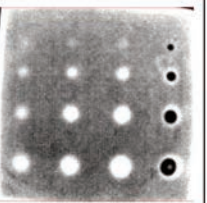
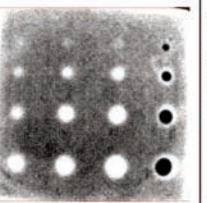
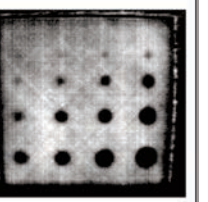
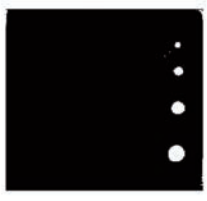
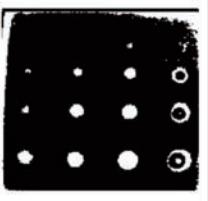
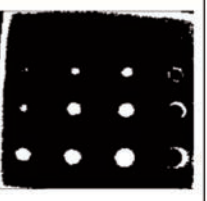
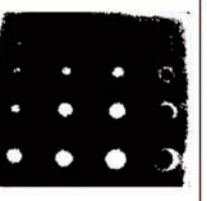
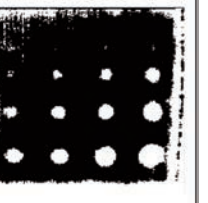
Pulsed Thermography(EchoTerm)				Step- Heating (C-CheckIR)
1,535s	14,384s	17,911s	19,026s	
				
				

Table 5 presents the images selected for analysis of the amount and size of damage. After binarization, images obtained using pulsed thermography allowed finding 14 out of 16 damages. Thus, damage detection efficiency in this study was at 88%. With step-heating thermography, 15 damages were found. Therefore the damage detection efficiency in this case was 94%.

Based on the distance between the centres of the damages and the number of pixels corresponding to this value, the diameters of damages were calculated proportionally in two directions x and y. The list of values calculated with errors in relation to the actual damage size is presented in Table 6. In order to better illustrate the results, the data is presented in the form of diagrams.

Table 6. Comparison of calculated damage diameters.

		Step- Heating (C-CheckIR)				Pulsed Thermography (EchoTerm)			
Dept h of hole	Real size [mm 	x [mm]	y [mm]	Δx [mm]	Δy [mm]	x [mm]	y [mm]	Δx [mm]	Δy [mm]
A	Ø16	25	24,47	9	8,47	16,3	15,96	0,3	0,04
	Ø12	19,57	19,15	7,57	7,15	11,96	11,7	0,04	0,3
	Ø8	14,13	14,89	6,13	6,89	7,61	8,51	0,39	0,51
	Ø4	2,17	4,26	1,83	0,26	5,43	5,32	1,43	1,32
B	Ø16	20,65	20,21	4,65	4,21	17,39	17,02	1,39	1,02
	Ø12	16,3	14,89	4,3	2,89	11,96	12,77	0,04	0,77
	Ø8	11,96	11,7	3,96	3,7	8,7	8,51	0,7	0,51
	Ø4	2,17	2,13	1,83	1,87	5,43	4,26	1,43	0,26
C	Ø16	16,3	18,09	0,3	2,09	16,3	17,02	0,3	1,02
	Ø12	14,13	12,77	2,13	0,77	13,04	12,77	1,04	0,77
	Ø8	8,7	8,51	0,7	0,51	7,61	7,45	0,39	0,55
	Ø4	1,09	1,06	2,91	2,94	-	-	-	-
D	Ø16	17,39	15,96	1,39	0,04	14,13	14,89	1,87	1,11
	Ø12	13,04	11,7	1,04	0,3	7,61	7,45	4,39	4,55
	Ø8	4,35	5,32	3,65	2,68	2,17	2,13	5,83	5,87
	Ø4	-	-	-	-	-	-	-	-
		Sum		96,16mm		Sum		38,14mm	

With pulsed thermography, image analysis allows a relatively accurate determination of the extent of damage compared to the actual size. The highest error values were recorded for the deepest defects. This difference is caused by the low contrast on the thermograms.

With step-heating thermography, the measured damages' sizes in most cases were much larger than the actual sizes. The total measurement error in this technique is almost three times greater than for pulsed thermography. However, it should be noted that this technique allows for finding more damages. In addition, the measurement was carried out on one thermogram and showed damage at various depths. For this reason heat diffusion around the damage had a greater impact.

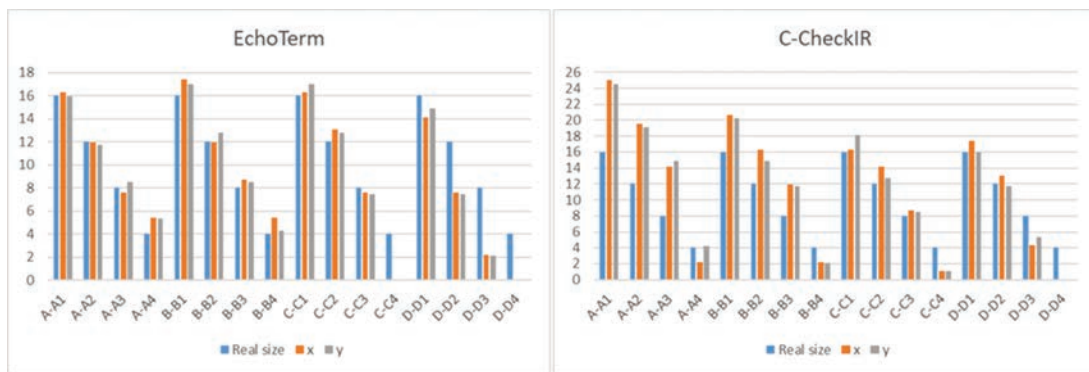


Figure 8. Diagrams showing the results of damage size measurement.

DISCUSSION

The paper presents general relations that occur during thermographic tests. The focus was on active thermography using the pulsed and step-heating techniques. They were used to carry out non-destructive testing of samples made of glass fibre reinforced polymer composite. These types of materials are often used in the aviation industry (radar screens).

The main advantages of both techniques are associated with using the contactless measuring systems and the detector which response time is relatively short. This significantly reduces the duration of tests even for large aircraft structures. The measuring systems are equipped with specialized IT and hardware tools, which enables the transition of the thermographic signals and leads to enhanced quality and accuracy of analyzing the test results recorded.

The possibility of using cooling curves in pulsed thermography is very important. It allows recording damages at different depths in different times. In addition, the ability to process thermograms using differentiation contributed to acquiring satisfactory results. It has also been observed that the contrast between undamaged and defective areas decreases over time. In consequence, the edges of deeper damages are blurred, making the smallest damage difficult or simply impossible to detect.

In the step-heating technique the thermogram stabilizes over time. This makes it possible to get very good quality of thermograms where a large number of defects are visible, regardless of their depth. Thus, it can be concluded that the pulsed technique is

better suited to detecting damages located closer to the surface, while the step-heating technique allows detection of damage which is deeper in the material.

A similar number of damages was found using both techniques. However, it should be pointed out that in step-heating thermography the images didn't undergo additional mathematical operations. Analysis of damage size after binarization showed that using step-heating thermography measurement was burdened with more than twice the error.

CONCLUSIONS

The results obtained lead to the following conclusions:

- Thermographic measurements allow detection of defects at various depths.
- The advantages of both techniques are: no contact with the surface of the test object and a fast response of the detector.
- In both methods selected are thermograms on which the surface of indications of damages was the largest.
- Both methods allow obtaining indications of flat-bottomed holes at all depths.
- In both techniques, the deepest damage was not found.
- Mathematical operations performed on thermograms in pulsed thermography allow enhancing the accuracy of defect assessment.
- In the pulsed technique, the contrast decreases with time (signal-to-noise ratio decreases), while in step-heating the image stabilizes with time making it possible to observe damages located deeper in the material.
- In the step-heating thermography, the raw image analysis was conducted. Despite this fact a similar number of damages was found with both techniques.
- Measurement of damage size on binarized images in the step-heating technique is burdened with a much larger error than in the pulsed technique.

REFERENCES

- [1] Lewinska-Romicka, A. (2001) *Badania nieniszczące. Podstawy defektoskopii*. Warszawa: WNT-PWN.
- [2] Kapuscinski, J., Lindeman, Z., Witemberg-Perzyk, D., Wojciechowski, S. and Boczkowska, A. (2003). *Kompozyty*. Warszawa: OWPW.
- [3] Swiderski, W. (2009). Nondestructive testing methods and techniques of composite materials by IR thermography, *Problemy Techniki Uzbrojenia*, 38(112), pp. 75-92, (in Polish).
- [4] Kornas, L. and Dragan, K., (2013). Zastosowanie termografii impulsowej w badaniach nieniszczących materiałów w konstrukcjach lotniczych, *XIX Seminarium Nieniszczące Badania Materialow*, Zakopane, 12-15 marca 2013, pp. 29-38.
- [5] Swiderski, W. and Vavilov, V. (2009). Determination of Thermo-physical Characteristics of Materials by IR Thermography Methods, *Biuletyn Wojskowej Akademii Technicznej*, Vol. 58, no 3, pp. 149-168, (in Polish).
- [6] Vedula, S., (2010). Infrared thermography and ultrasonic inspection of adhesive bonded structures, overview and validity. All Theses. 890.
https://tigerprints.clemson.edu/all_theses/890

- [7] Oliferuk, W. (2008). *Termografia podczerwieni w nieniszczących badaniach materiałów i urządzeń*, Warszawa: Biuro Gamma.
- [8] Vavilov, V. P. and Burleigh, D. D. (2015). Review of pulsed thermal NDT: Physical principles, theory and data processing, *NDT & E International*, Vol. 73, pp. 28-52. 10.1016/j.ndteint.2015.03.003.
- [9] Roche, J. M. and Balageas, D. (2015). Common tools for quantitative pulse and step-heating thermography – Part II: Experimental investigation, *Quantitative InfraRed Thermography Journal*. 12. 10.1080/17686733.2014.996341
- [10] <https://www.thermalwave.com/products/#EchoTherm>
- [11] Steven, M. and Shepard, S. (2007). Flash Thermography of Aerospace Composites, *V Conferencia Panamericana de END* Buenos Aires – Octubre 2007.